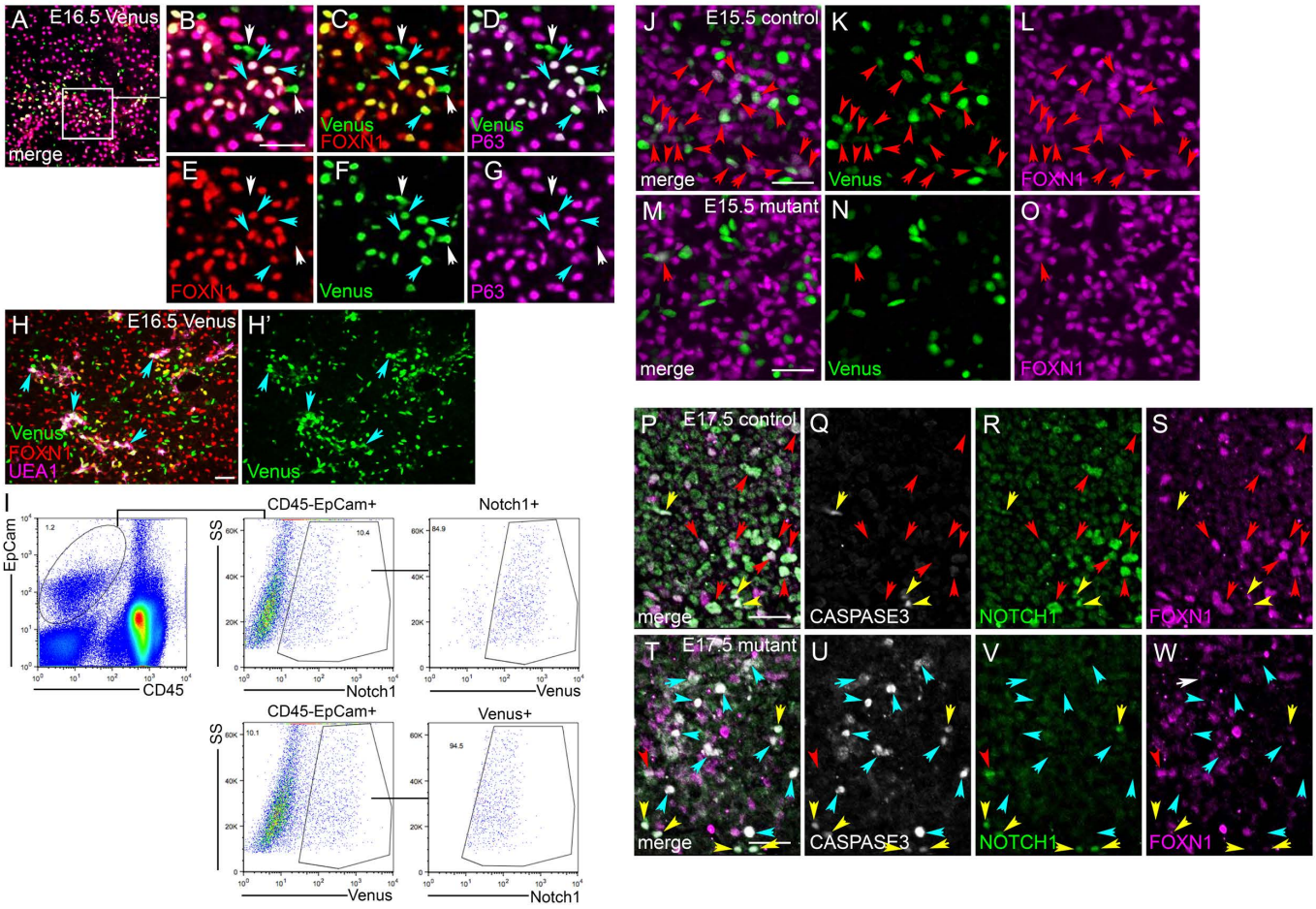

Figure S1. Venus signal is reduced in TECs after *Notch1* deletion. (A-G) Immunofluorescence of E16.5 *CBF:H2B-Venus* thymus for expression of Venus (green), P63 (magenta) and Foxn1 (red). Box in (A) is zoomed area in (B-G). White arrows indicate Venus^{+};P63^{-}FOXN1^{-} cells; cyan arrows indicate Venus^{+};P63^{+}FOXN1^{+} cells. (H) Immunofluorescence of E16.5 *CBF:H2B-Venus* thymus for expression of Venus (green), Foxn1 (red) and UEA1 (magenta). Cyan arrows indicate Venus^{+};UEA1^{+}FOXN1^{+} cells. (I) Flow cytometric analysis of TECs from E17.5 *CBF:H2B-Venus* thymus stained for CD45, EpCam, Notch1-IC and expression of Venus. (J-O) Immunofluorescence of E15.5 *CBF:H2B-Venus* only control (J-L) and *Foxn1^{Cre};Notch1$^{fx/fx}$;CBF:H2B-Venus* mutant (M-O) thymus for expression of Venus (green) and Foxn1 (magenta). Red arrows indicate Venus^{+};FOXN1^{+} cells. (P-W) Immunofluorescence of E17.5 Cre- control (P-S) and *Foxn1^{Cre};Notch1$^{fx/fx}$* mutant (T-W) thymus for expression of Caspase 3 (white), NOTCH1-IC (green), and Foxn1 (magenta). Red arrows indicate Notch1-IC^{+};FOXN1^{+};Caspase3^{-} cells; cyan arrows indicate Notch1-IC^{-};FOXN1^{-};Caspase3^{+}cells; yellow arrows indicate Notch1-IC^{+};FOXN1^{-};Caspase3^{+} cells. Scale bars, 20 μm.

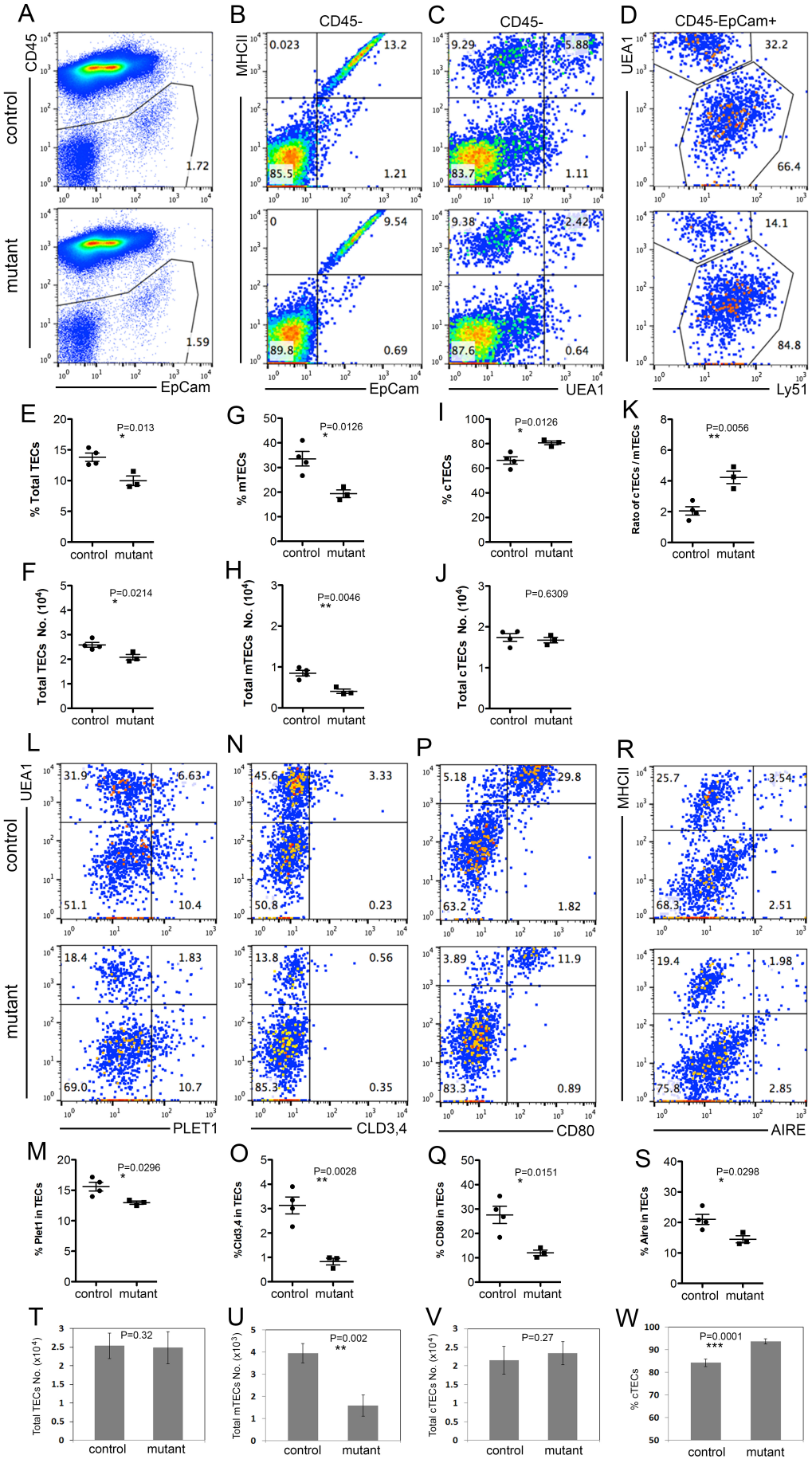

Figure S2. mTEC differentiation after *Notch1* deletion from TECs. Flow cytometric analysis of mTEC markers for cells from digested newborn *Foxn1*^{Cre};*Notch1*$^{fx/fx}$ mutant and Cre- control thymi. (A) Total thymus cells stained for CD45 and EpCam. (B) CD45- gate stained for EpCam and MHCII. (C) CD45^{-} cells stained for UEA1 and MHCII. (D) CD45^{-} EpCam^{+} TECs stained for UEA1 and Ly51. (E) Percentage of TECs in mutant and control thymi at newborn stage. (F) Total number of TECs in mutant and control thymi at newborn stage. (G) Percentage and (H) Total number of mTECs in mutant and control thymi. (I) Percentage and (J) Total number of cTECs in mutant and control thymi. (K) The ratio of cTECs/mTECs in mutant and control thymi. (L) CD45^{-} EpCam^{+} TECs stained for UEA1 and Plet1. (M) Percentage of Plet1^{+} mTECs in mutant and control thymi. (N) CD45^{-} EpCam^{+} TECs stained for UEA1 and CLD3,4. (O) Percentage of CLD3,4^{+} TECs in mutant and control thymi. (P) CD45^{-} EpCam^{+} TECs stained for UEA1 and CD80. (Q) Percentage of CD80^{+} TECs in mutant and control thymi. (R) CD45^{-} EpCam^{+} TECs stained for Aire. (S) Percentage of Aire^{+} TECs in mutant and control thymi. (T) Total number of TECs in mutant and control thymi at E17.5 stage. (U) Total number of mTECs in mutant and control thymi at E17.5 stage. (V) Total number and Percentage (W) of cTECs in mutant and control thymi at E17.5 stage. ***$P \leq 0.0005$. **$P \leq 0.005$. *$P \leq 0.05$. $n \geq 3$.

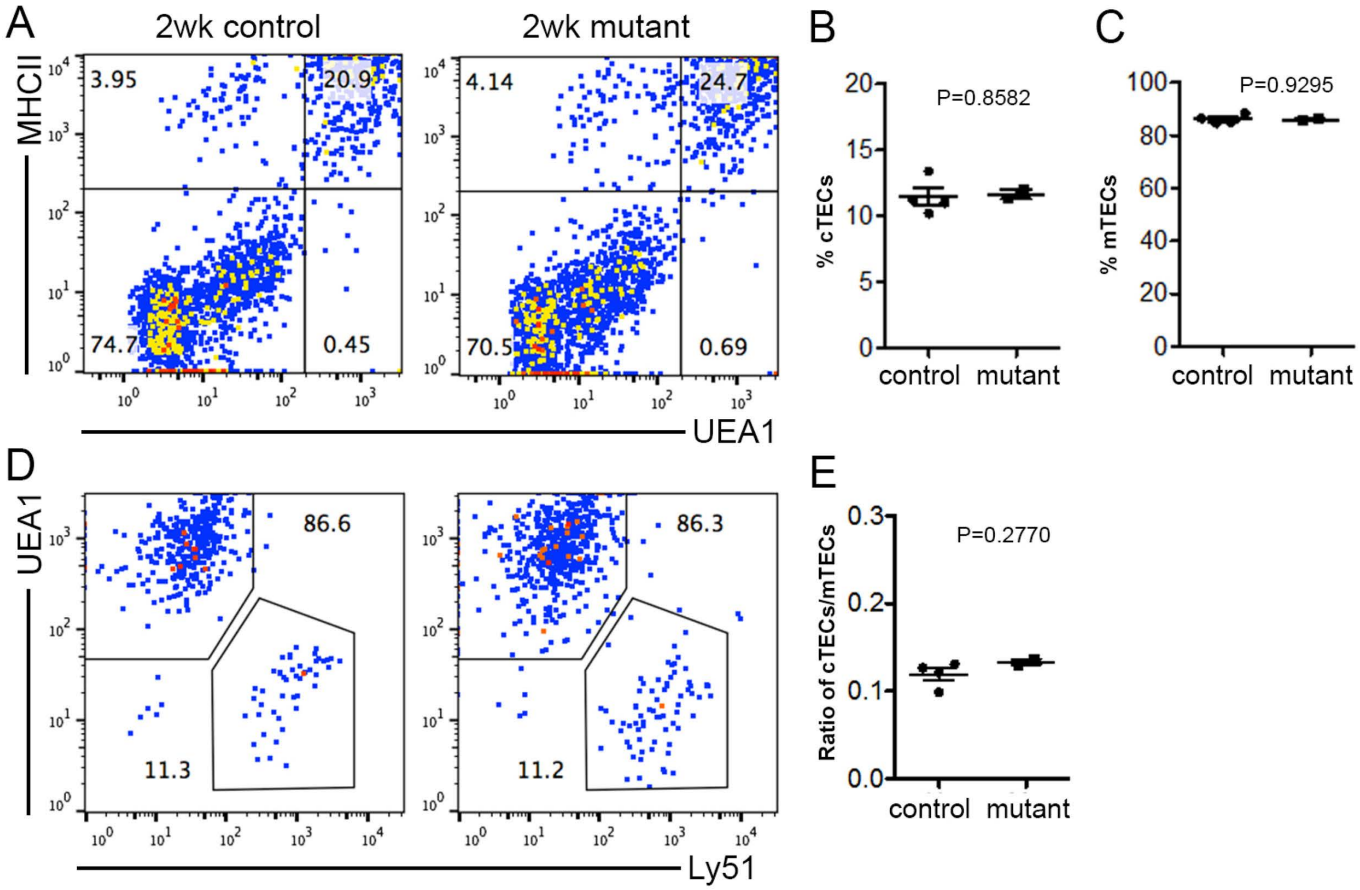

Figure S3. TEC differentiation after *Notch1* deletion at postnatal stage. Flow cytometric analysis of TEC from 2 week old Cre- control and *Foxn1*^{Cre};*Notch1*$^{fx/fx}$mutant thymus. (A) CD45^{-} cells stained for UEA1 and MHCII. (B) Percentage of cTECs in mutant and control thymi. (C) Percentage of mTECs in mutant and control thymi. (D) CD45^{-} EpCam^{+} TECs stained for UEA1 and Ly51. (E) The ratio of cTECs/mTECs in mutant and control thymi. n ≥ 3.

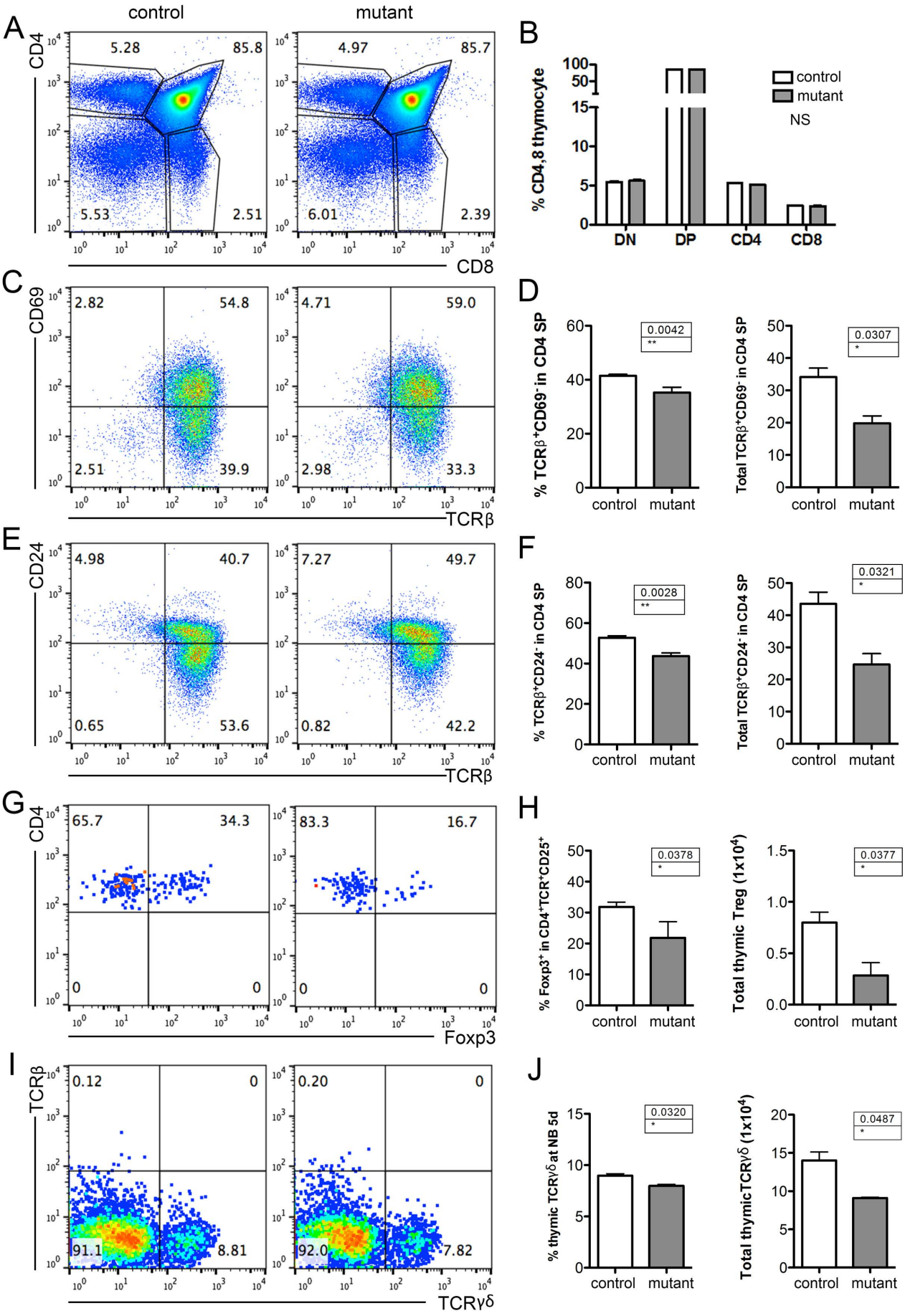

Figure S4. *Notch1* deletion from TECs affects αβT cells, γδT cells and regulatory T cells in thymus. Flow cytometric analysis of thymocytes from postnatal day 5 *Foxn1*^{Cre};*Notch1*$^{fx/fx}$ mutant and Cre- control thymi. (A) Total thymocytes stained for CD4 and CD8. (B) Percentages of major subsets defined by CD4 and 8 expression. (C) CD4 SP thymocytes stained for CD69 and TCRβ. (D) Percentage and total number of TCRβ^{+} thymocytes in CD4^{+}CD69^{-} subpopulation. (E) CD4^{+} SP thymocytes stained for CD24 and TCRβ. (F) Percentage and total number of TCRβ^{+} thymocytes in the CD4^{+}CD24^{-} subpopulation. (G) CD4^{+}CD25^{+}TCRβ^{+} thymocytes stained for Foxp3. (H) Percentage and total number of Foxp3^{+} thymocytes in the CD4^{+}CD25^{+}TCRβ^{+} subpopulation. (I) CD4^{-}CD8^{-} thymocytes stained for TCRβ and TCRγδ. (J) Percentage and total number of TCRγδ^{+} thymocytes in the CD4^{-}CD8^{-}TCRβ^{-} subpopulation. $^{**}P \leq 0.005$. $^{*}P \leq 0.05$. $n \geq 3$.

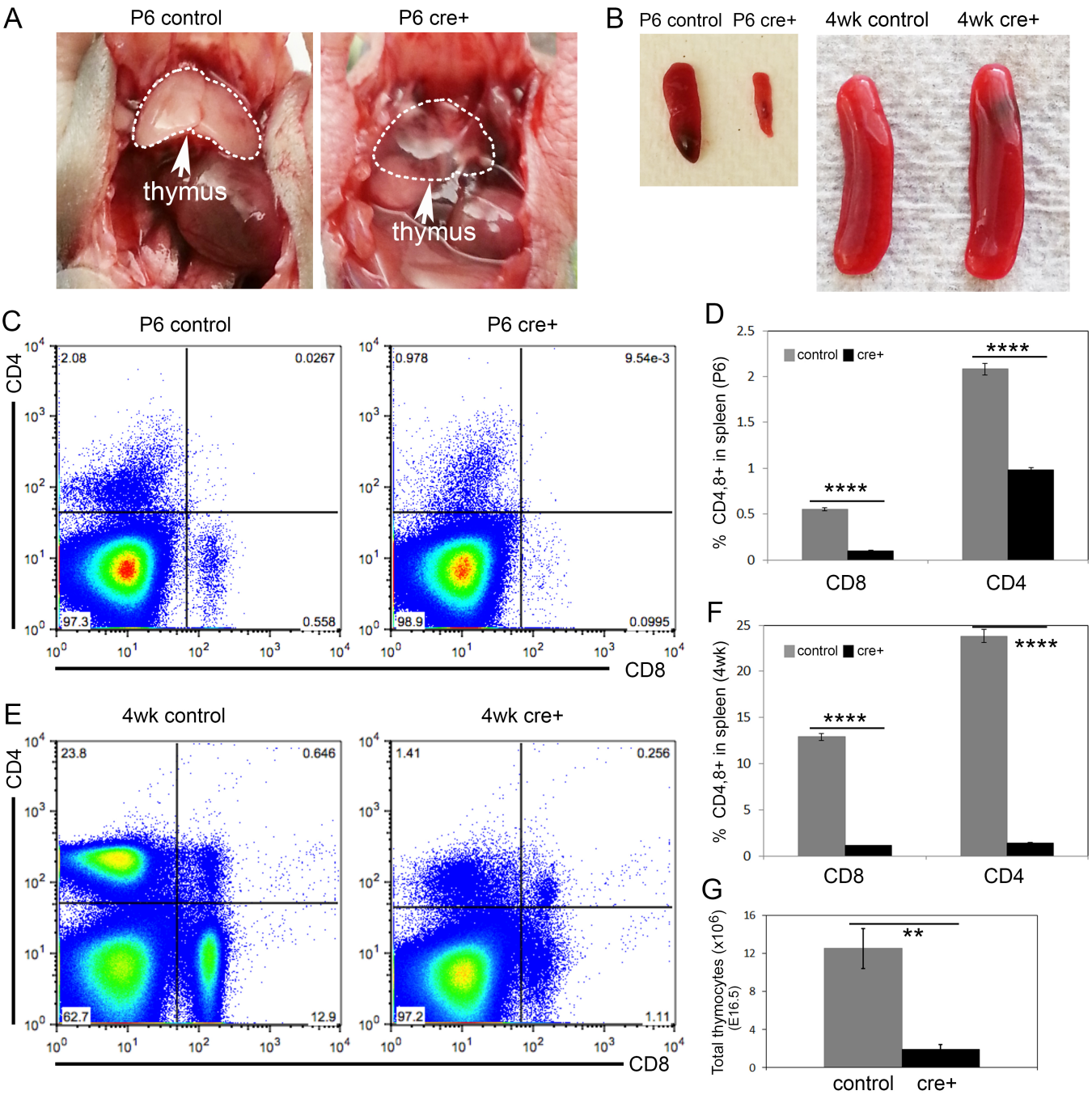

Figure S5. Forced NOTCH1 signaling in all TECs induces diminishment of thymic tissue and affects T cell phenotypes at postnatal stages. Postnatal phenotypes of *Foxn1*$^{+/Cre}$;*Rosa*$^{N1\text{-}IC}$ and Cre- control mice (A) Pictures of postnatal day 6 (P6) thymus *in situ*. (B) Spleens from P6 (left panel) and 4 week (right panel) mice. (C) Flow cytometric analysis of splenic cells from P6 mice stained for CD4 and CD8. (D) Percentage of $CD4^+$ and $CD8^+$ cells in P6 spleen. (E) Flow cytometric analysis of splenic cells from 4 week mice stained for CD4 and CD8. (F) Percentage of $CD4^+$ and $CD8^+$ cells in 4 week spleen. (G) Total thymocyte numbers in E16.5 *Foxn1*$^{+/Cre}$;*Rosa*$^{N1\text{-}IC}$ and Cre- control embryos. $^{**}P \leq 0.005$. $^{****}P \leq 0.0001$. $n \geq 3$.

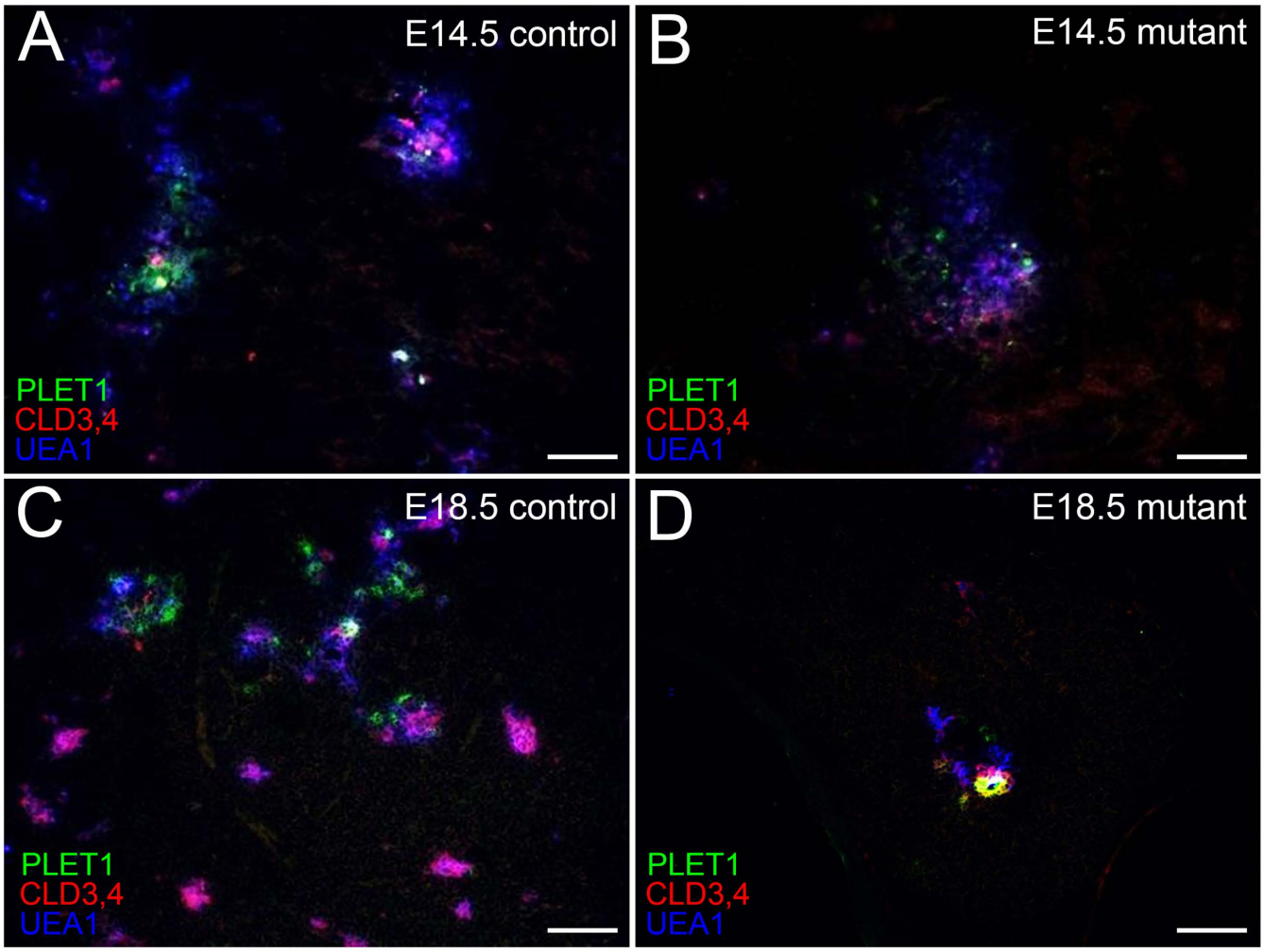

Figure S6. Fewer TEPCs in the *Foxg1^{Cre};Notch1$^{fx/fx}$* fetal thymus. Immunofluorescence of E14.5 (A,B) and E18.5 (C,D) *Foxg1^{Cre};Notch1$^{fx/fx}$* mutant (B,D) and control (A,C) thymus for expression of CLD3,4 (red), PLET1 (green) and UEA1 (blue). Scale bars, 50 μm. n > 3.

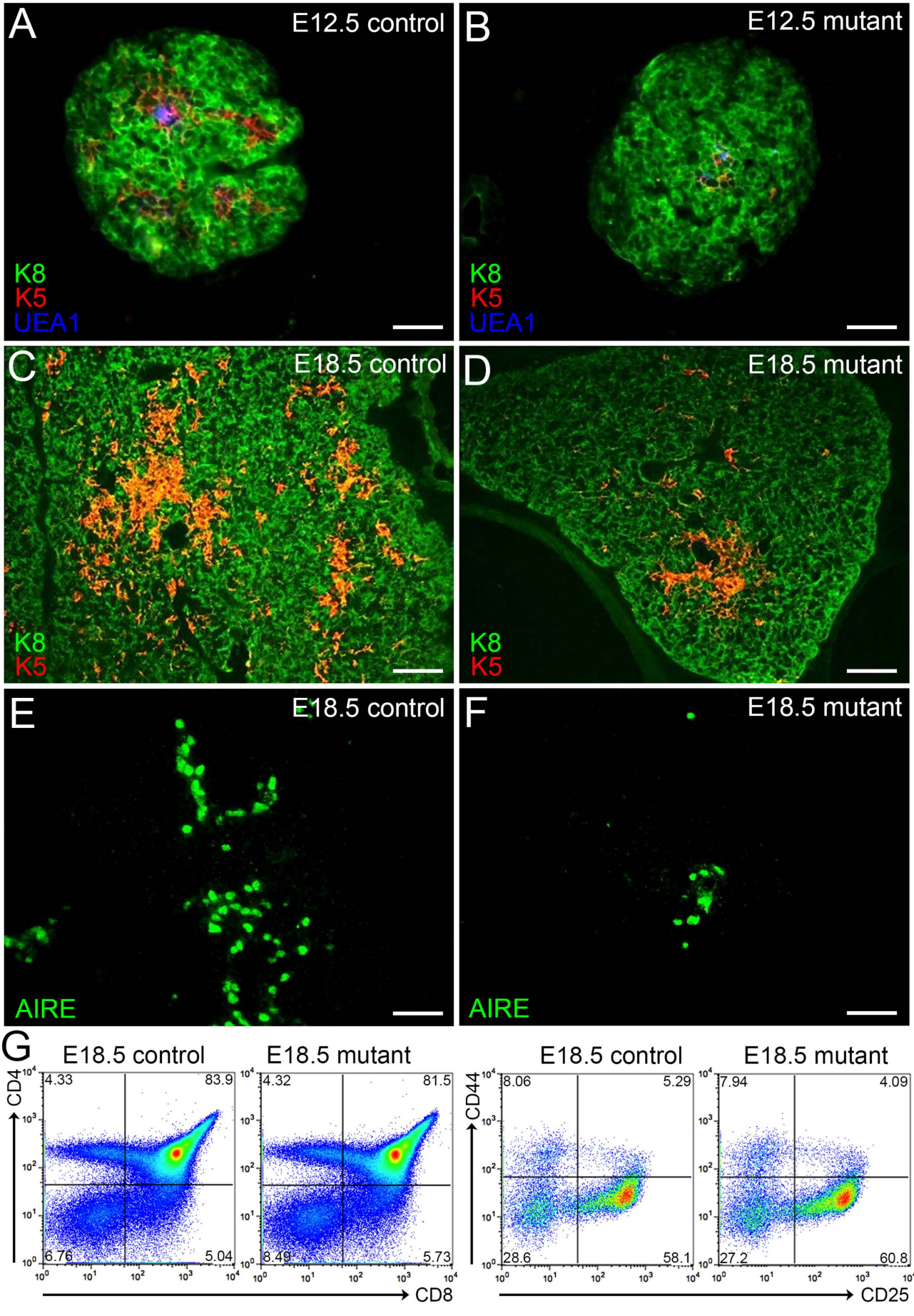

Figure S7. TEC organization and differentiation are affected in the *Foxg1^{Cre};Notch1$^{fx/fx}$* fetal thymus. (A,B) Immunofluorescence of E12.5 *Foxg1^{Cre};Notch1$^{fx/fx}$* mutant (B) and control (A) thymus for expression of K5 (red), K8 (green) and UEA1 (blue). (C,D) Immunofluorescence of E18.5 *Foxg1^{Cre};Notch1$^{fx/fx}$* mutant (D) and control (C) thymus for expression of K5 (red), K8 (green). (E,F) Immunofluorescence of E18.5 *Foxg1^{Cre};Notch1$^{fx/fx}$* mutant (F) and control (E) thymus for expression of AIRE. (G) Flow cytometric analysis of intrathymic thymocytes isolated from E18.5 *Foxg1^{Cre};Notch1$^{fx/fx}$* mutant and control thymi stained for CD4, CD8, CD44 and CD25 subsets. Scale bars, 50 μm. n > 3 for IHC; n > 5 for flow cytometry.

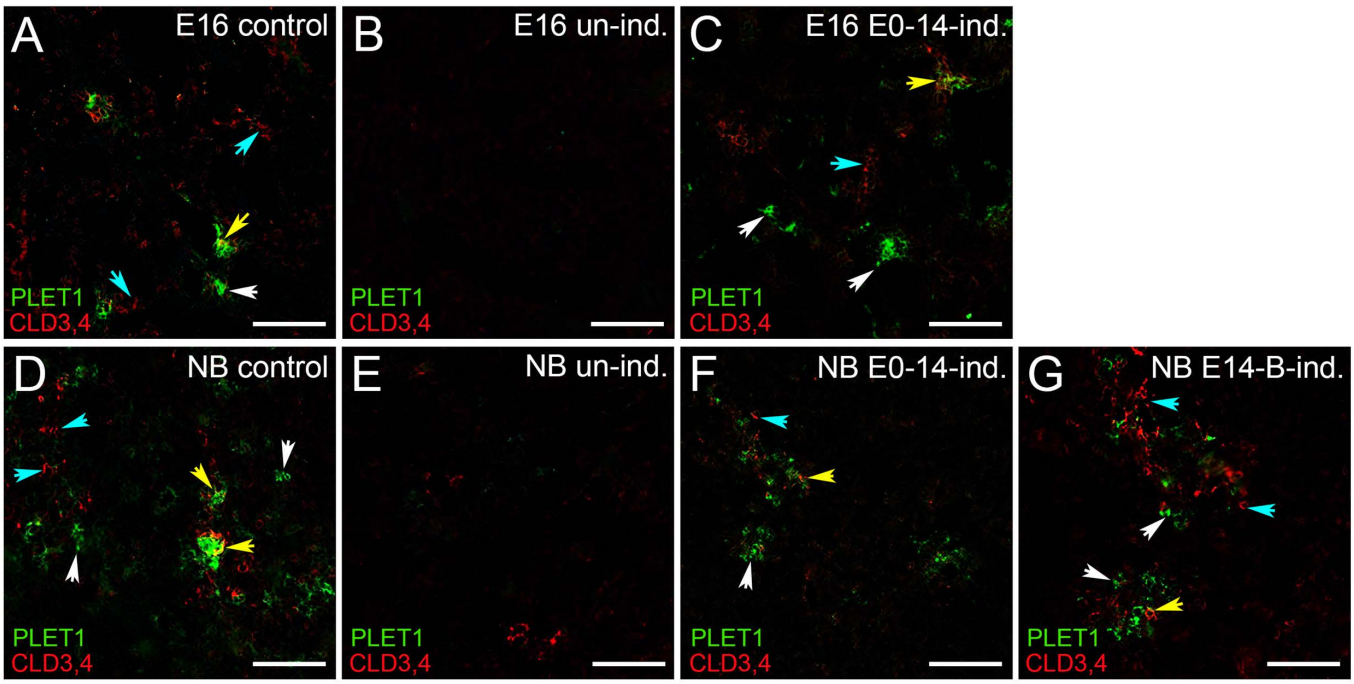

Figure S8. Restoring NOTCH signaling receptivity in TECs rescues mTEPC generation. (A-D) Immunofluorescence of E16 (A-C) or NB (D-G) thymi collected from controls RBPj$^{fx/+}$;Foxn1^{Cre};Rosa^{rtTA};Tet^{on}-RBPj-HA (A, D), uninduced RBPj$^{fx/fx}$;Foxn1^{Cre};Rosa^{rtTA};Tet^{on}-RBPj-HA (RBPJ^{ind}) (B, E), or RBPJ^{ind} mice injected with doxycycline from E0-14 (C, F) or from E14-NB (G), as in Figure 7. Thymi are stained for expression of CLD3,4 (red) and PLET1 (green). White arrows indicate PLET1^{+};CLD3,4^{-} cells; cyan arrows indicate PLET1^{-};CLD3,4^{+} cells; yellow arrows indicate PLET1^{+};CLD3,4^{+} cells. Compare with Figure 2. Scale bars: 50 µm.

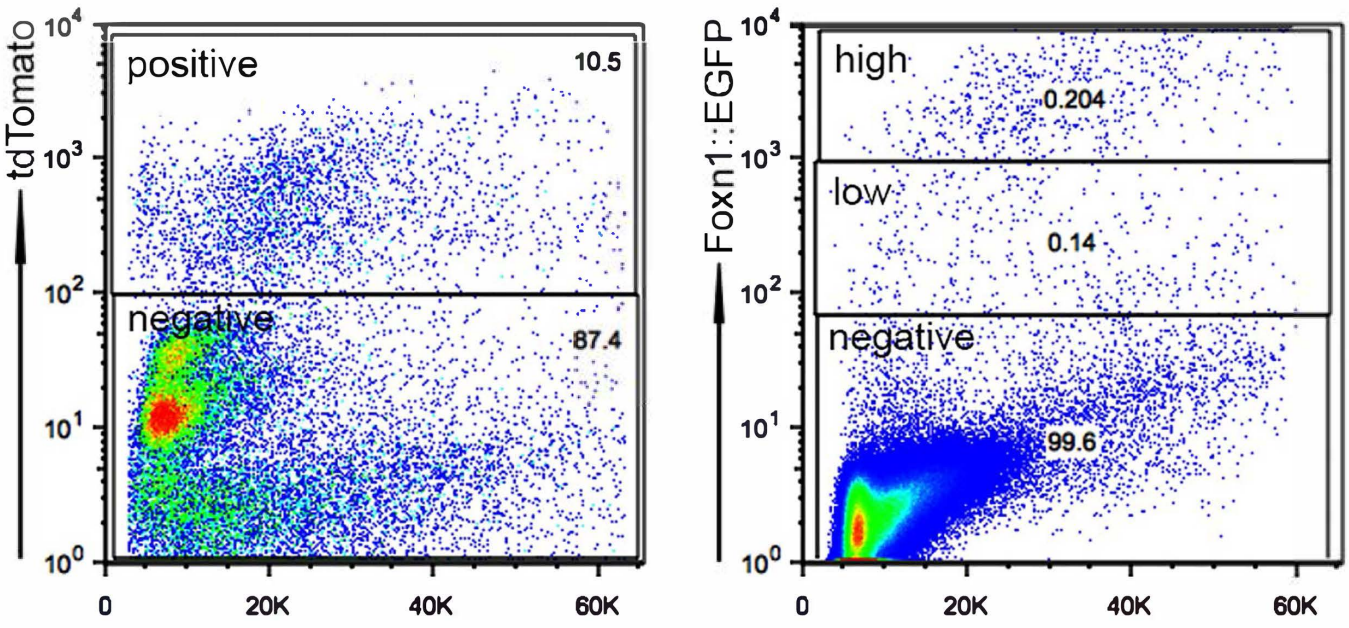

Figure S9. Gating controls for flow cytometric analysis of thymic cells isolated from newborn N1IP::Cre^{LO};tdTomato;Foxn1::EGFP and N1IP::Cre^{HI};tdTomato;Foxn1::EGFP mice. Cells were divided into FOXN1 high, low, and very low/negative for the analyses shown in Figures 6 and 7 based on these gates.